Li *et al. Complex Eng Syst* 2023;3:15
DOI: 10.20517/ces.2023.15

Complex Engineering Systems

Research Article

Open Access

Model predictive control of multi-objective adaptive cruise system based on extension theory

Zhutao Li[1], Xinxin Zhao[1], Jue Yang[1], Menglei Liu[1]

[1]Vehicle Engineering, University of Science and Technology Beijing, Beijing 100080, China.

Correspondence to: Dr. Xinxin Zhao, Vehicle Engineering, School of Mechanical Engineering, University of Science and Technology Beijing, No.30 Xueyuan Road, Haidian District, Beijing 100080, China. E-mail: xinxinzhao@ustb.edu.cn

How to cite this article: Li Z, Zhao X, Yang J, Liu M. Model predictive control of multi-objective adaptive cruise system based on extension theory. *Complex Eng Syst* 2023;3:15. http://dx.doi.org/10.20517/ces.2023.15

Received: 18 May 2023 **First Decision:** 3 Jul 2023 **Revised:** 12 Jul 2023 **Accepted:** 29 Aug 2023 **Published:** 13 Sep 2023

Academic Editor: Hamid Reza Karimi **Copy Editor:** Fanglin Lan **Production Editor:** Fanglin Lan

Abstract

Under certain working conditions, the car-following performance and longitudinal ride comfort of adaptive cruise control (ACC) vehicles are contradictory. Therefore, the extension coordinated control is introduced into the weighted design of each performance index under the model predictive control (MPC) framework to optimize the overall vehicle driving performance. In this article, the dynamic model of the ACC vehicle and the variable time headway model are established, and then the predictive model and its corresponding cost function under the MPC framework are designed. By using the co-simulation platform of CarSim and Matlab/Simulink, three different simulation conditions are established and compared with the traditional ACC operating results. It was determined that the tracking speed error in the acceleration stage can be reduced by approximately 40% and the acceleration amplitude can be reduced by between 8%–17%. Therefore, there is an optimization effect under this control method. This study provides a foundation for curving ACC under an extension coordinated control theory.

Keywords: Extension coordinated control, adaptive cruise control, model predictive control, advanced driver assistance systems

1. INTRODUCTION

With the development of the automotive industry, the advanced driver assistance system (ADAS) has become a key research direction for various institutions aimed at improving ride comfort, safety, and fuel economy

© The Author(s) 2023. **Open Access** This article is licensed under a Creative Commons Attribution 4.0 International License (https://creativecommons.org/licenses/by/4.0/), which permits unrestricted use, sharing, adaptation, distribution and reproduction in any medium or format, for any purpose, even commercially, as long as you give appropriate credit to the original author(s) and the source, provide a link to the Creative Commons license, and indicate if changes were made.

during vehicle operation. Among them, the adaptive cruise control (ACC) has become a focal point of researchers due to its wide range of applications. In recent years, in order to achieve energy conservation and emission reduction, the consideration criteria of vehicle fuel economy, ride comfort, and driving safety have been integrated into the design of the ACC system. At the same time, in order to reduce the incidence of traffic accidents caused by driver fatigue, integrating ACC into driverless vehicles has become a promising solution. Yin *et al.* established the objective function based on an optimal control theory and verified the effectiveness of the algorithm on straight and curved roads[1]. Compared with the traditional PID control method, model predictive control (MPC) can better meet the control precision of unmanned vehicles and complicated driving conditions, and it is more fit with the nonlinear characteristic of the vehicles[2]. To improve the safety, comfort, and fuel economy of the ACC system, Qu *et al.* proposed a multi-mode switching intelligent driving longitudinal ACC strategy[3]. In order to improve the performance of autonomous vehicles in path tracking, Wang *et al.* combined a fuzzy adaptive weight control theory to design a new MPC controller[4]. Vasebi *et al.* presented a holistic literature review of energy-optimal adaptive cruise control algorithms which provided a useful insight into the development of this research field[5]. However, when the ACC vehicle needs to meet better following performance, it may adopt larger acceleration and deceleration to meet the following distance requirements, which leads to poor ride comfort and fuel economy. In this case, a single control method could not adapt to the time variability of the environment; that is, the traditional fixed weight matrix could not meet the requirements, so extension control is introduced to coordinate this deficiency under the multi-objective MPC framework[6]. Zhao *et al.* from Nanjing University of Aeronautics and Astronautics designed an extensible controller to effectively handle the conflict between control output and control effect in extreme operating conditions[7]. In the traditional lane keeping system, global-region control adopts a single control algorithm, which often leads to poor control of some control areas. In order to solve this problem, Wang *et al.* used extension control theory combined with Takagi-Sugeno-Kang fuzzy control to create a new controller for the system[8]. Under the background of multi-objective control, the extension theory uses the correlation evaluation of the system characteristic state and the optimization of the control parameters by the correlation degree and then divides the measurement mode to realize the multi-region switching control, thus improving the control precision and performance. Under traditional fixed matrix control conditions for multi-objective ACC, in order to achieve better following performance, it leads to poor riding comfort and fuel economy. The main contributions of this article with respect to this issue are the following twofold.

- An MPC controller and cost function based on the motion state relationship between the host vehicle and the preceding vehicle and extension coordinated control theory were established.

- A correlation function was introduced for comfort, fuel economy, and other objectives to form a real-time weighted matrix for optimization. The feasibility and effectiveness of the control method were verified through joint simulation using Matlab/Simulink and Carsim.

The remainder of this paper is organized as follows. The adaptive cruise vehicle model is established in Section 2. Multi-target adaptive cruise under extension control is described in Section 3. In Section 4, simulation results are illustrated, and the conclusion is described in Section 5.

2. ADAPTIVE CRUISE VEHICLE MODEL

2.1. Variable time headway model

In the theory of variable time headway (VTH), it is believed that the time headway τ is influenced by environmental variables. In this paper, it is established that when the relative speed between two vehicles is constant, the time headway should be increased when the preceding vehicle decelerates and decreased when the preceding vehicle accelerates[9].

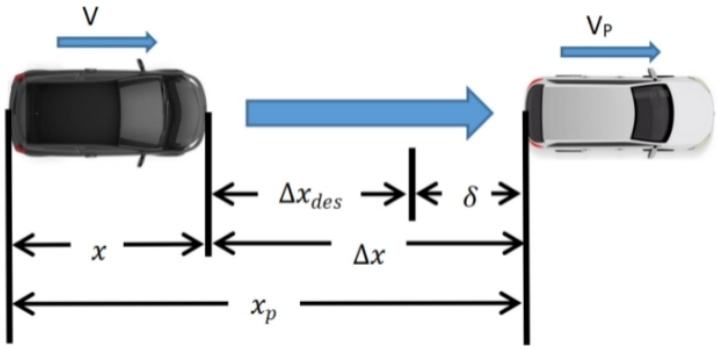

Figure 1. Longitudinal following diagram.

Therefore, the calculation formula is designed as follows:

$$\tau = \tau_0 - a * (v_p - v) - b * a_p \tag{1}$$

In the formula, a_p stands for acceleration of the preceding vehicle, v_p stands for the speed of the preceding vehicle, v stands for the speed of the host vehicle, τ_0 represents the default time headway, set to 1.5s; a and b are parameters set to 0.3 and 1.5, respectively. Meanwhile, the upper and lower limits of the time headway are considered, with a range of 1.4-2.2s.

2.2. Longitudinal dynamic model

The corresponding mechanical balance equation can be established for the vehicle in the longitudinal direction:

$$F_d = m * a_x + m * g * f * \cos\theta + m * g * \sin\theta + \frac{1}{2} * \rho * C_D * A * v_x^2 \tag{2}$$

Where F_d represents the longitudinal force of the tire, m represents the mass of the vehicle, g represents the gravitational acceleration, f represents the coefficient of friction of the road, θ represents the road slope, a_x represents the longitudinal acceleration of the vehicle, ρ represents the air density, C_D represents the air resistance coefficient, A represents the frontal area, and v_x represents the longitudinal velocity of the vehicle[10].

3. MULTI-TARGET ADAPTIVE CRUISE UNDER EXTENSION CONTROL

3.1. Model predictive control

3.1.1. Prediction model

The kinematic models for the host vehicle and the preceding vehicle can be expressed as follows[11]:

$$\begin{cases} \Delta x(k) = x_p(k) - x(k) \\ \Delta x_{des}(k) = \Delta x_0(k) + \tau v(k) \\ \delta(k) = \Delta x(k) - \Delta x_{des}(k) \end{cases} \tag{3}$$

Here, Δx represents the actual following distance, Δx_{des} represents the desired following distance, x_p represents the position of the preceding vehicle, x represents the position of the host vehicle, k represents the discrete time index, and δ represents the error between the actual following distance and the desired following distance[12]. The dynamic model is shown in Figure 1.

$$\begin{cases} a(k) = \dfrac{v(k) - v(k-1)}{T_s} \\ j(k) = \dfrac{a(k) - a(k-1)}{T_s} \end{cases} \tag{4}$$

where $a(k)$ represents the acceleration of the host vehicle at time k, $j(k)$ represents the acceleration change rate at time k, and T_s stands for the discrete sampling period[13], which is represented by the calculation step size in Matlab.

Under discrete conditions, the state variables based on kinematics can be selected as distance, relative velocity, host speed, host acceleration, and the rate of change of host acceleration, which can be expressed as follows[14]:

$$\Delta x(k+1) = \Delta x(k) - v_{rel}(k) * T_s + \frac{1}{2} * a(k) * T_s^2 \tag{5}$$

$$v_{rel}(k+1) = v_{rel}(k) + a_p(k) * T_s - a(k) * T_s \tag{6}$$

$$v(k+1) = v(k) + a(k) * T_s \tag{7}$$

$$a(k+1) = (1 - \frac{T_s}{t}) * a(k) + \frac{T_s}{t} * u(k) \tag{8}$$

$$j(k+1) = \frac{-1}{t} * a(k) + \frac{1}{t} * u(k) \tag{9}$$

v_{rel}represents the relative velocity between two vehicles, a_p represents the acceleration of the preceding vehicle, t represents the control time constant, and u represents the desired acceleration.

In this paper, the disturbance variable is chosen as the acceleration of the preceding vehicle, and the state variables are selected as relative distance, host vehicle speed, relative speed, acceleration, and acceleration change rate[15]: $x(k) = [\Delta x(k), v(k), v_{rel}(k), a(k), j(k)]^{\mathrm{T}}$. The system output variables are the relative distance error, relative velocity, acceleration, and acceleration change rate: $y(k) = [\delta(k), v_{rel}(k), a(k), j(k)]^{\mathrm{T}}$. Based on the selected state and output variables, the predictive model can be established as follows:

$$x(k+1) = Ax(k) + Bu(k) + Gw(k) \tag{10}$$

$$y(k) = Cx(k) - Z \tag{11}$$

where A, B,G,C, and Z are system state-space matrices.

$$A = \begin{bmatrix} 1 & 0 & T_s & -\frac{1}{2}T_s^2 & 0 \\ 0 & 1 & 0 & T_s & 0 \\ 0 & 0 & 1 & -T_s & 0 \\ 0 & 0 & 0 & 1 - \frac{T_s}{t} & 1 \\ 0 & 0 & 0 & -\frac{1}{t} & 0 \end{bmatrix}, B = \begin{bmatrix} 0 \\ 0 \\ 0 \\ \frac{T_s}{t} \\ \frac{1}{t} \end{bmatrix}, G = \begin{bmatrix} \frac{1}{2}T_s^2 \\ 0 \\ T_s \\ 0 \\ 0 \end{bmatrix}, C = \begin{bmatrix} 1 & -\tau & 0 & 0 & 0 \\ 0 & 0 & 1 & 0 & 0 \\ 0 & 0 & 0 & 1 & 0 \\ 0 & 0 & 0 & 1 & 0 \end{bmatrix}, Z = \begin{bmatrix} \Delta x_0 \\ 0 \\ 0 \\ 0 \end{bmatrix}$$

In this paper, the reference trajectory[16] is defined as:$y_r(k) = 0.95 * I_i d$, where $I_i d$ stands for identity matrix, $y_r(k) = [\delta_{ref}(k), v_{rel_ref}(k), a_{ref}(k), j_{ref}(k)]^{\mathrm{T}}$, where $\delta_{ref}(k)$ represents the reference value of relative distance error, v_{rel_ref} represents the reference value of relative velocity, $a_{ref}(k)$ represents the reference value of acceleration, and $j_{ref}(k)$ represents the reference value of acceleration change rate. The standard form of the discrete linear MPC prediction model is:

$$\widehat{X}_p(k+p|k) = \overline{A}x(k) + \overline{B}U(k+m) + \overline{G}W(k+p) + \overline{H}e_x(k) \tag{12}$$

$$\widehat{Y}_p(k+p|k) = \overline{C}x(k) + \overline{D}U(k+m) + \overline{E}W(k+p) + \overline{F}e_x(k) - \overline{Z} \tag{13}$$

In these equations, p represents the prediction time horizon, and m represents the control time horizon. $\widehat{X}_p(k+p|k)$ and $\widehat{Y}_p(k+p|k)$ represent the predicted values of the state and output variables at future time $k+p$, based on the information available at time k, respectively. e_x represents the set of outputs of the system, that is,

the expected acceleration. $W(k+p)$ represents the error between the actual and predicted values of the state variables. represents the disturbance matrix[17].

$$\widehat{X}_p(k+p|k)=\begin{bmatrix}\widehat{x}_p(k+1|k)\\ \widehat{x}_p(k+2|k)\\ \vdots\\ \widehat{x}_p(k+p|k)\end{bmatrix},\widehat{Y}_p(k+p|k)=\begin{bmatrix}\widehat{y}_p(k+1|k)\\ \widehat{y}_p(k+2|k)\\ \vdots\\ \widehat{y}_p(k+p|k)\end{bmatrix},U(k+m)=\begin{bmatrix}u(k)\\ u(k+1)\\ \vdots\\ u(k+c-1)\end{bmatrix},W(k+p)=\begin{bmatrix}w(k)\\ w(k+1)\\ \vdots\\ w(k+p-1)\end{bmatrix}$$

$$e_x=x(k)-x(k-1)$$

$\overline{A}$, $\overline{B}$, $\overline{G}$, $\overline{H}$, $\overline{C}$, $\overline{D}$, $\overline{E}$, $\overline{F}$, and $\overline{Z}$ are the discrete matrices, and the correlation coefficient matrices are given as follows[18]:

$$\overline{A}=\begin{bmatrix}A\\ A^2\\ \vdots\\ A^{p-1}\end{bmatrix}_{p*1},\overline{B}=\begin{bmatrix}B & 0 & \dots & 0\\ AB & B & \dots & \vdots\\ \dots & \dots & \vdots & 0\\ A^{p-1}B & A^{p-2}B & \dots & \sum_{l=0}^{p-c}A^lB\end{bmatrix}_{p*c},\overline{G}=\begin{bmatrix}G & 0 & \dots & 0\\ AG & G & \dots & \vdots\\ \dots & \dots & \vdots & 0\\ A^{p-1}G & A^{p-2}G & \dots & G\end{bmatrix}_{p*p}$$

$$\overline{H}=\begin{bmatrix}H_1\\ H_2\\ \vdots\\ H_P\end{bmatrix}_{p*1},\overline{C}=\begin{bmatrix}CA\\ CA^2\\ \vdots\\ CA^{p-1}\end{bmatrix}_{p*1},\overline{D}=\begin{bmatrix}CB & 0 & \dots & 0\\ CAB & CB & \dots & \vdots\\ \dots & \dots & \vdots & 0\\ CA^{p-1}B & CA^{p-2}B & \dots & \sum_{l=0}^{p-c}CA^lB\end{bmatrix}_{p*c}$$

$$\overline{E}=\begin{bmatrix}CG & 0 & \dots & 0\\ CAG & CG & \dots & \vdots\\ \dots & \dots & \vdots & 0\\ CA^{p-1}G & CA^{p-2}G & \dots & GCG\end{bmatrix}_{p*p},\overline{F}=\begin{bmatrix}CH_1\\ CH_2\\ \vdots\\ CH_P\end{bmatrix}_{p*1},\overline{Z}=\begin{bmatrix}Z\\ Z\\ \vdots\\ Z\end{bmatrix}_{p*1}$$

3.1.2. Performance index

For longitudinal following performance, a safe following distance must be guaranteed[19]:

$$\Delta x(k)=x_p(k)-x(k)\geq d_s \tag{14}$$

In the process of driving, the acceleration of the host vehicle and the change rate of acceleration can be selected as the evaluation indices for the ride comfort. While driving, the smaller the change in the rate of acceleration, the better the ride comfort. In the case of fuel economy, the acceleration of the host vehicle is the main affecting factor. Generally, during the driving process, the smoother the speed change, the higher the fuel economy. Therefore, it is advisable to minimize the time required for the vehicle to undergo significant longitudinal acceleration or deceleration during the following process and reduce the amplitude of the acceleration change rate, which can effectively improve the fuel economy of vehicles. Therefore, the following indicators exist:

$$v_{min}\leq v(k)\leq v_{max} \tag{15}$$

$$a_{min}\leq a(k)\leq a_{max} \tag{16}$$

$$j_{min}\leq j(k)\leq j_{max} \tag{17}$$

3.1.3. Cost function

The multi-objective optimization problem is converted into a quadratic programming problem by linear weighting.

$$J = q_\delta(\delta - \delta_{ref})^2 - q_v(v_{rel} - v_{rel,ref})^2 + q_a(a - a_{ref})^2 + q_j(j - j_{ref})^2 \tag{18}$$

Where q_δ stands for the weight of relative distance error, q_v stands for the weight of relative velocity, q_a stands for the weight of acceleration, and q_j stands for the weight of acceleration change rate.

After eliminating terms that are irrelevant to control variables, the cost function of the established prediction model can be expressed as:

$$\begin{aligned} J = 2\{x^T(k)[\overline{C}^T - C^T\overline{\Phi}^T]\overline{QD} + W(k+p)^T\overline{E}^T\overline{QD} - [\overline{Z}^T - Z^T\overline{\Phi}^T]\overline{QD} + ex(k)^T\overline{F}^T\overline{QD}\} \\ * U(k+c) + U(k+c)^T(\overline{R} + \overline{D}^T\overline{QD})U(k+c) \end{aligned} \tag{19}$$

Here, Q is the weighting coefficient matrix for the output variables[20], $Q = diag(q_\delta, q_v, q_a, q_j)$, and R is the weighting coefficient for the control variables.

By incorporating the performance indices as constraints into the predictive model, the following expressions are obtained:

$$\begin{cases} \overline{M} \le \overline{L}\widehat{X}_p(k+p) \le \overline{N} \\ U(k+m) \le U_{max} \\ -U(k+m) \le -Umin \end{cases} \tag{20}$$

The coefficient matrices in the above equation are:

$$M = \begin{bmatrix} d_c \\ v_{min} \\ a_{min} \\ j_{min} \end{bmatrix}, N = \begin{bmatrix} \infty \\ v_{max} \\ a_{max} \\ j_{max} \end{bmatrix}, L = \begin{bmatrix} 1 & 0 & 0 & 0 & 0 \\ 0 & 1 & 0 & 0 & 0 \\ 0 & 0 & 1 & 0 & 0 \\ 0 & 0 & 0 & 10 & 1 \end{bmatrix}, U_{max} = \begin{bmatrix} u_{max} \\ \vdots \\ u_{max} \end{bmatrix}, U_{min} = \begin{bmatrix} u_{min} \\ \vdots \\ u_{min} \end{bmatrix}$$

$$\overline{M} = \begin{bmatrix} M \\ M \\ \vdots \\ M \end{bmatrix}_{p*1}, \overline{N} = \begin{bmatrix} N \\ N \\ \vdots \\ N \end{bmatrix}_{p*1}, \overline{L} = \begin{bmatrix} L & \dots & 0 \\ \vdots & \ddots & \vdots \\ 0 & \dots & L \end{bmatrix}$$

After rearrangement, the standard form of the quadratic programming can be obtained as follows[21]:

$$\begin{cases} min\{U(k+m)^T K_1 U(k+m) + 2K_2 U(k+m)\} \\ s.t.\Omega U(k+m) \le T \end{cases}, \text{where } K_1 = \overline{R} + \overline{D}^T\overline{QD},$$

$$K_2 = \{x^T(k)[\overline{C}^T - C^T\overline{\Phi}^T]\overline{QD} + W(k+p)^T\overline{E}^T\overline{QD} - [\overline{Z}^T - Z^T\overline{\Phi}^T]\overline{QD} + ex(k)^T\overline{F}^T\overline{QD}\},$$

$$\Omega = \begin{bmatrix} \overline{LB} \\ -\overline{LB} \\ I \\ -I \end{bmatrix}, T = \begin{bmatrix} \overline{N} - \overline{LG}W(k+p) - \overline{LA}x(k) - \overline{LH}e_x(k) \\ -\overline{M} + \overline{LG}W(k+p) + \overline{LA}x(k) + \overline{LH}e_x(k) \\ Umax \\ -Umin \end{bmatrix}$$

3.2. Extension control

3.2.1. Partition of characteristic variables and extension sets

It is essential to ensure the longitudinal performance stability of the ACC system mentioned in this paper before considering ride comfort, fuel economy, and other factors. Therefore, when the longitudinal following state is not within an acceptable range, it is necessary to adjust the weight matrix of MPC. Based on actual driving experience, it is known that the impact on passengers caused by the relative distance between two vehicles is

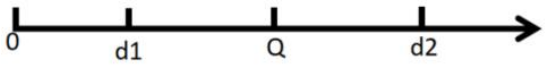

Figure 2. One-dimensional extension set of following distance error.

more significant than the relative vehicle speed[22]. Therefore, in this paper, the longitudinal following error is chosen as the characteristic variable, and the weight q_δ is adjusted further while setting q_v, q_a, q_j to constant values. As a result, the evaluation criteria are that when the longitudinal following distance error is small, it indicates that the ACC system's following ability is strong; when the following distance error is large, it indicates that the ACC system's following ability is weak.

As shown in Figure 2, a one-dimensional extension set is established, and the boundary values of the classical domain and the extension domain are defined as d_1 and d_2, respectively. According to the definition of the extension domain, d_2 is specified as the maximum allowable value of the following distance error. The boundary value of the classical domain is usually the smaller value, so their calculation formulas are as follows:

$$d_2 = d_{max} * SDE^{-1} \tag{21}$$

$$d_1 = 0.1 * d_2 \tag{22}$$

$$SDE^{-1} = k_{SDE} v_x + d_{SDE} \tag{23}$$

where SDE^{-1} represents the sensitivity of the intelligent vehicle to the following distance error, and the values of the relevant parameters are selected based on driver test data[23]:$d_{max} = 7.2m$,$k_{SDE} = 0.06$,$d_{SDE} = 0.12m$.

3.2.2. Calculate correlation degree

In the theory of extension control, it is believed that the correlation degree $K(S) = 0$ and $K(S) = -1$ reflect qualified and unqualified responses to whether a feature variable can be accepted[24]. In the case of the longitudinal following distance error, the point of zero indicates the absence of the following distance error and is also the ideal point of this feature variable. Additionally, the extensible distance is defined as the distance from a point to a set. As shown in Figure 3, the classical domain is $< O, d_1 >= X_c$, and the extensible domain is $< d_1, d_2 >= X_e$. Therefore, the distance from point Q to the classical domain is defined as $\rho(Q, X_c)$, and the distance from point Q to the extensible domain is defined as $\rho(Q, X_e)$:

$$\rho(Q, X_c) = \begin{cases} -|Od_1|, Q \in < O, d_1 > \\ |Od_1|, Q \in < d_1, +\infty > \end{cases} \tag{24}$$

$$\rho(Q, X_e) = \begin{cases} -|Od_2|, Q \in < O, d_2 > \\ |Od_2|, Q \in < d_2, +\infty > \end{cases} \tag{25}$$

$$\begin{cases} K(S) = \dfrac{\rho(Q, X_e)}{D(Q, X_e, X_c)} \\ D(Q, X_e, X_c) = \rho(Q, X_e) - \rho(Q, X_c) \end{cases} \tag{26}$$

3.2.3. Real-time weight design

According to the value of the correlation degree $K(S)$, the measurement pattern can be divided as follows:

$$\begin{cases} M_1 = \{S | K(S) > 1\} \\ M_2 = \{S | 0 < K(S) < 1\} \\ M_3 = \{S | K(S) < 0\} \end{cases} \tag{27}$$

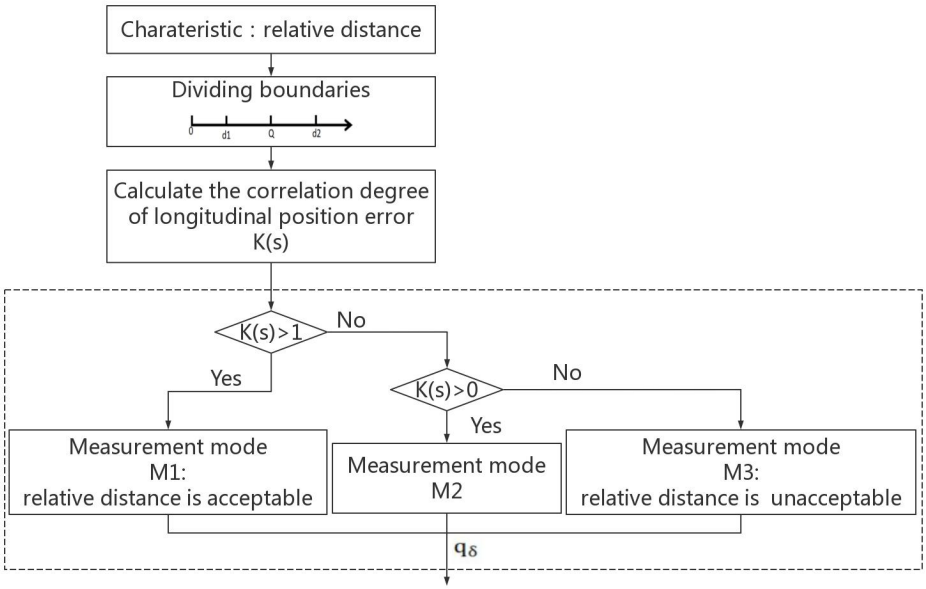

Figure 3. Measurement mode recognition flowchart.

The symbolsM_1, M_2, and M_3 correspond to the classic domain, expandable domain, and non-domain, respectively. When the following distance error is in M_1, it indicates that the error is acceptable and the weight does not need to be adjusted. When it is in M_2, it means the error is about to exceed the limit and the weight needs to be adjusted promptly. When in M_3, it means the error is unacceptable and the weight must be increased immediately to meet system requirements[25]. Figure 3 shows the calculation process of the measurement modes.

Therefore, the real-time weight calculation formula can be designed as follows:

$$q_\delta = \begin{cases} 0.3, K(S) > 1 \\ 0.3 + 0.4 * (1 - K(S)), 0 < K(S) < 1 \\ 0.4, K(S) < 0 \end{cases} \tag{28}$$

3.3. Lower controller

First, an inverse engine model is established, assuming that the vehicle is traveling on a straight road with a zero slope[26]:

The vehicle driving equation is as follows:

$$F_t = F_f + F_w + F_j \tag{29}$$

Where F_t represents driving force, F_f represents rolling resistance, F_w represents air resistance, and F_j represents acceleration resistance. Furthermore, $T_{des} = F_t * \frac{r_{eff}}{i_g i_0 \eta_T}$, which can be obtained after unfolding:

$$T_{des} = \frac{(mgf + \frac{1}{2} C_D A \rho v^2 + \delta m a_{des}) r_{eff}}{i_g i_0 \eta_T} \tag{30}$$

$$\delta = 1 + \frac{1}{m} \frac{\sum I_w}{r^2} + \frac{1}{m} \frac{I_f i_g^2 i_0^2 \eta_T}{r^2} \tag{31}$$

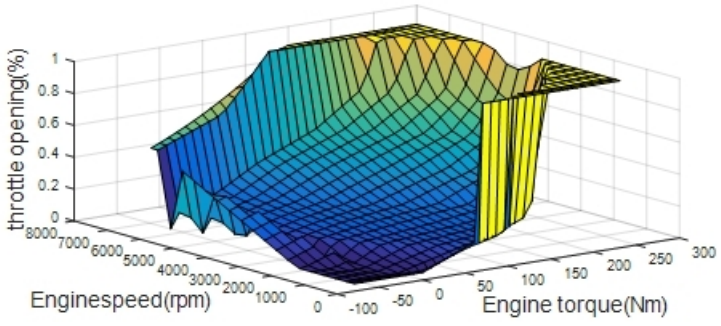

Figure 4. Throttle opening curve surface.

In the equation, T_{des} stands for desired engine torque, m stands for the total the vehicle mass, g stands for the gravitational acceleration, f stands for the road friction coefficient, C_D stands for the air resistance coefficient, A stands for the frontal area,δ stands for the rotational mass conversion coefficient, r_{eff} stands for the effective radius of the wheel, i_g stands for the transmission ratio of the gearbox[27], i_0 stands for the transmission ratio of the main reducer, η_T stands for the transmission efficiency, I_f stands for the rotational inertia of the flywheel, and I_w stands for rotational inertia of the wheel[28].

Based on the throttle opening curve shown in Figure 4, the current expected throttle opening can be obtained from the expected torque and engine speed and output to the vehicle model.

Secondly, an inverse brake model is established, assuming a linear relationship between the brake master cylinder pressure and the braking torque[29]: The magnitude of braking torque can be derived from the resistance torque function:

$$F_{br} = F_f + F_w + F_j \tag{32}$$

F_{br}represents the sum of the braking forces acting on the wheels, and there is $T_{br} = F_{br} * r_{eff}$. Therefore:

$$T_{br} = r_{eff}(\delta m a_{des} - mgf - \frac{1}{2}C_D A\rho v^2) \tag{33}$$

$$P_{br} = T_{br}/K_1 \tag{34}$$

Where T_{br} stands for braking torque, P_{br} stands for brake pressure, and K_1 stands for the linearity coefficient. The next step is to establish the logic for switching between the accelerator and brake. Based on experimental data, the baseline for the switching logic can be obtained. In order to avoid frequent switching between the accelerator and brake and ensure the smoothness and fuel economy of the vehicle, we set threshold values for the accelerator and brake by shifting the curve up and down. The switching curve is shown in Figure 5.

4. RESULTS

4.1. Simulation condition settings

The E-type car in Carsim was selected for use in this paper, and the setting of vehicle parameters can be seen in Figure 6.

At the same time, the input variables of the Carsim interface are set as brake master cylinder pressure signals and open loop throttle control signals; output variables are relative distance, relative speed, host vehicle longitudinal speed, host vehicle acceleration, engine crankshaft spin, transmission gear ratio. The simulated road conditions are set to a straight track with a length of 500 meters, and the road friction coefficient is set to a constant value of 0.9. As shown in Figure 7, in the driver control section, the initial speed is set to 30 km/h, and

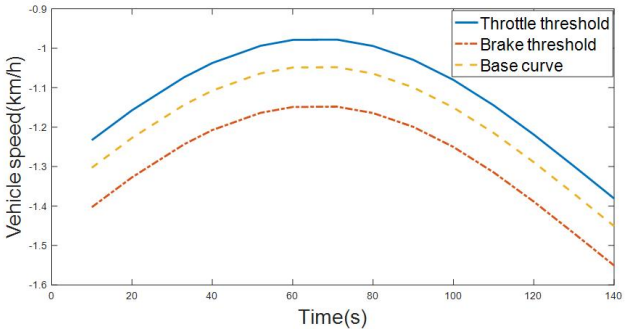

Figure 5. Throttle/brake switching logic diagram.

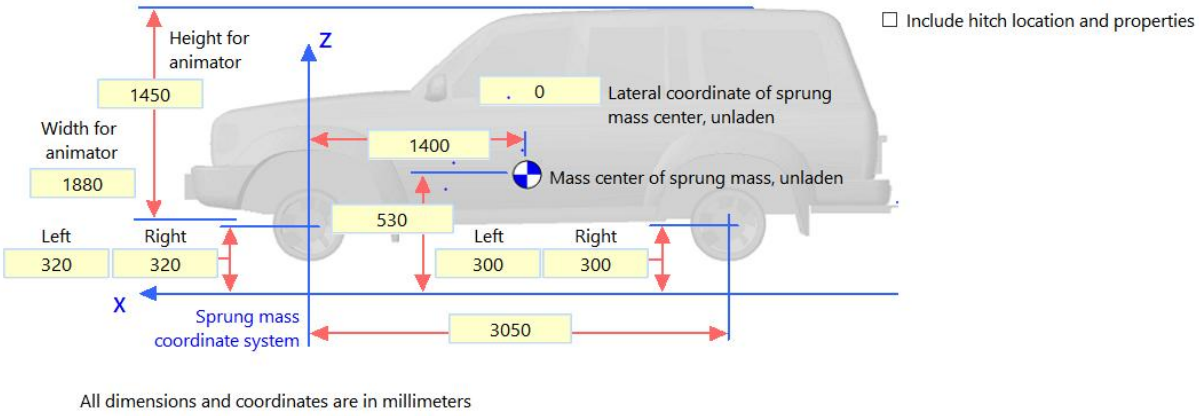

Figure 6. Parameters of vehicle model.

the brake control signal is provided by the upper controller, so it is set to a constant value of 0; the transmission is set to 6-speed transmission.

4.2. Analysis of simulation results

According to the previous introduction, the overall control structure is built, as shown in Figure 8.

Three distinct working conditions were set to verify the effectiveness of the proposed control method, and the control results under the traditional MPC were taken as the control. The simulation results are shown in Figures 9-11.

In working condition 1, the target speed is set as the sine curve between 30 km/h and 50 km/h. (A), (B), and (C) in Figure 9 show the variation curves of vehicle speed, the relative speed of the preceding and host vehicles, and the acceleration of the host vehicle, respectively. It can be seen from the speed curve that in the whole simulation process, the speed of the host vehicle controlled by an extension theory is closer to the speed curve of the target vehicle, with a maximum error of 0.6km/h. Furthermore, the relative speed of the two vehicles is smaller than that controlled under traditional MPC. The overall amplitude variation range is reduced by 50%, which indicates that the tracking effect of the host vehicle is better. In addition, it can be seen from the acceleration curve that the variation amplitude of vehicle acceleration under the extension control is smaller. Compared with the traditional MPC, the oscillation amplitude of acceleration is reduced by 8%; therefore, the ride comfort and fuel economy of the vehicle are also optimized. In the second condition, the speed of the preceding vehicle is set to accelerate to 50 km/h and maintained for 5 s, and then it changes between 30 km/h

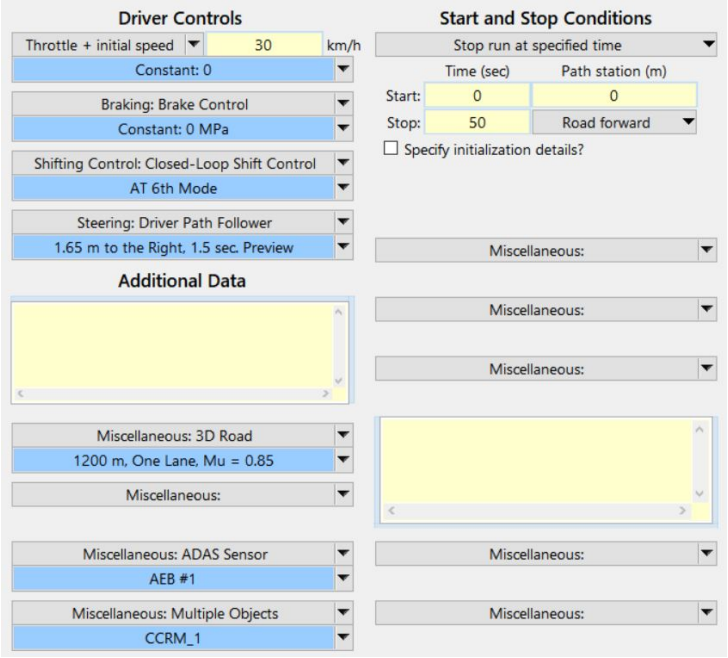

Figure 7. Settings of the host vehicle model.

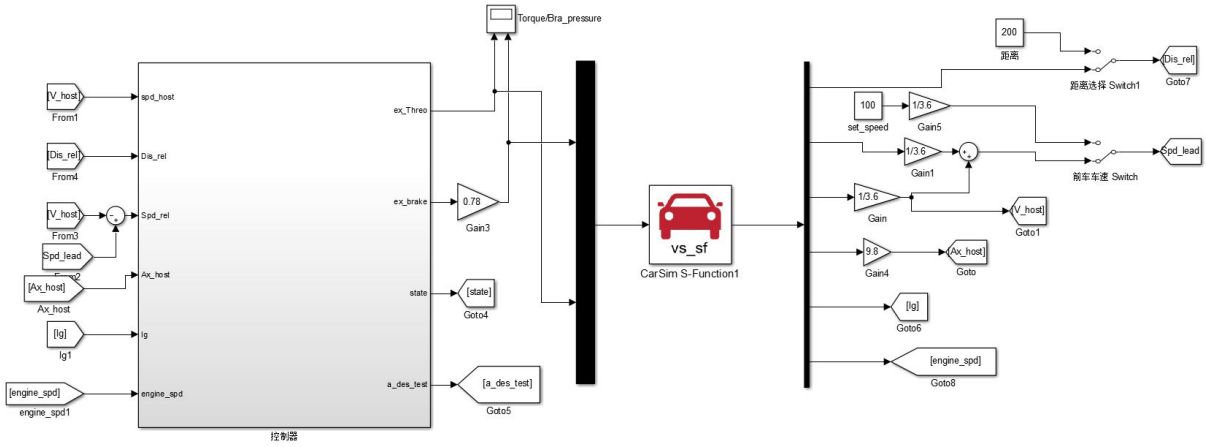

Figure 8. Model control structure.

and 50 km/h. It can be seen from the speed curve and relative speed curve that extension control has more advantages in tracking effect in the acceleration stage. The control method has a certain optimization effect, and the maximum error of tracking speed is 0.66km/h. However, in the deceleration stage, for example, the range of relative speed variation of 35–40 s is larger than that in the traditional MPC, and the range increases by 43%. This indicates that the control effect of extension control on relative distance error is not ideal under the current working conditions, so the extension control on relative speed can be considered to generate a new real-time weight matrix for further optimization.

In the third condition, the speed of the preceding vehicle was set to accelerate from 30 km/h to 50 km/h, and it remained unchanged in the following simulation process. It can be found that in the entire simulation process, the vehicle speed under the extension control is closer to the target speed, the maximum relative speed error is

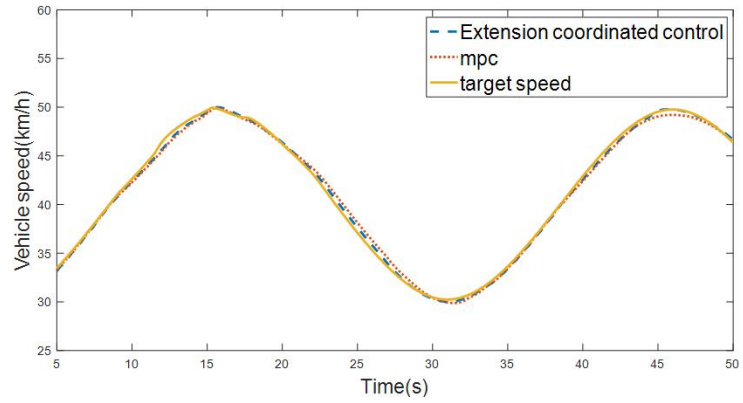

(a)

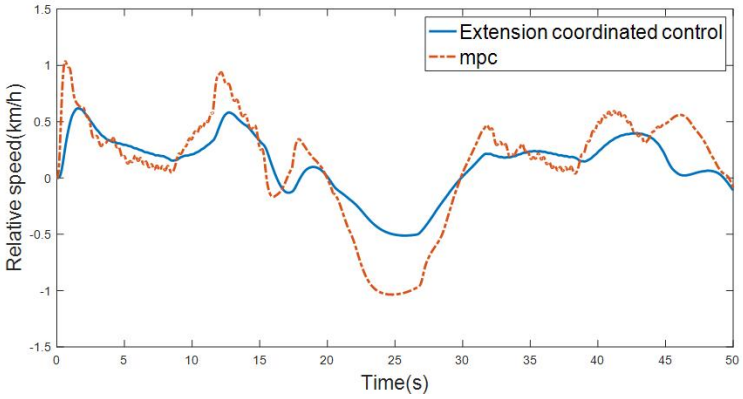

(b)

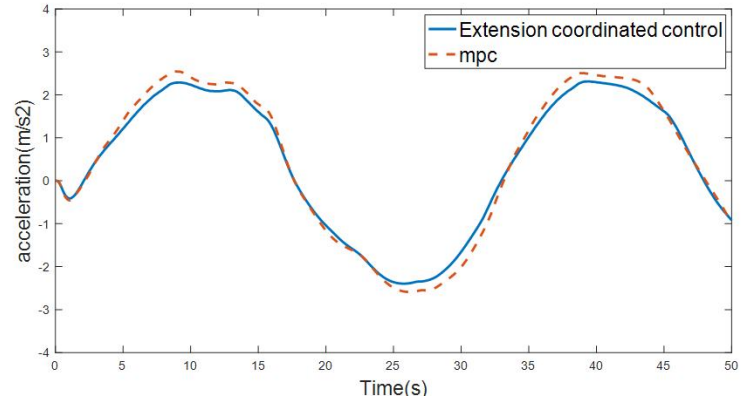

(c)

Figure 9. Simulation results of working condition No.1. a: condition No.1 vehicle speed; b: condition No.1 relative speed; c: condition No.1 acceleration.

0.64 km/h, and the variation range of relative speed and acceleration is reduced by 40% and 17%, respectively. The results show that when compared with the traditional MPC, there is an optimization effect, and the goal of multi-objective ACC is achieved. However, in the 35–50 s range, that is, the constant speed stage, the relative speed curve has a small amplitude of oscillation, which also appears in the acceleration curve. The amplitude increases by 20% compared with that controlled by the traditional MPC, indicating that the current control

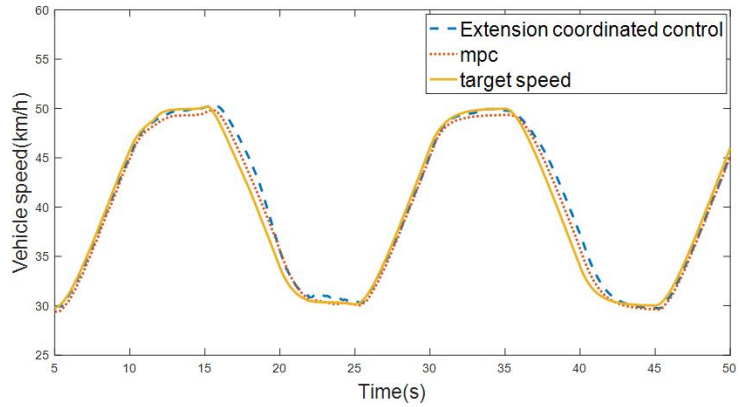

(a)

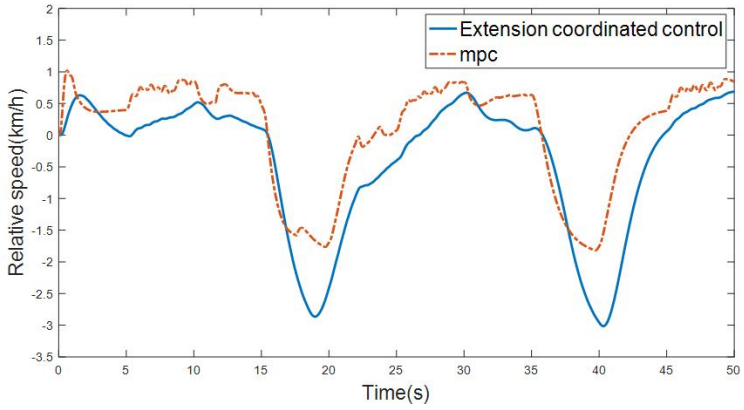

(b)

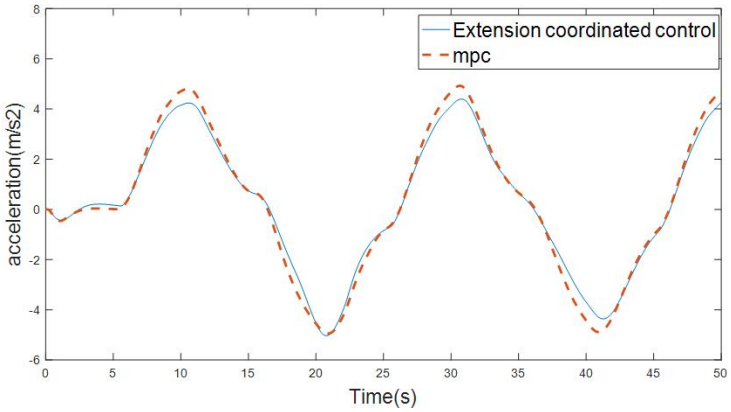

(c)

Figure 10. Simulation results of working condition No.2. a: condition No.2 vehicle speed; b: condition No.2 relative speed; c: condition No.2 acceleration.

method can improve the vehicle performance to a greater extent in the acceleration stage. However, under the condition of constant speed, the weight setting corresponding to the acceleration change rate needs to be updated. Therefore, an extension control theory should be applied to the corresponding state variable in future research to optimize the control results.

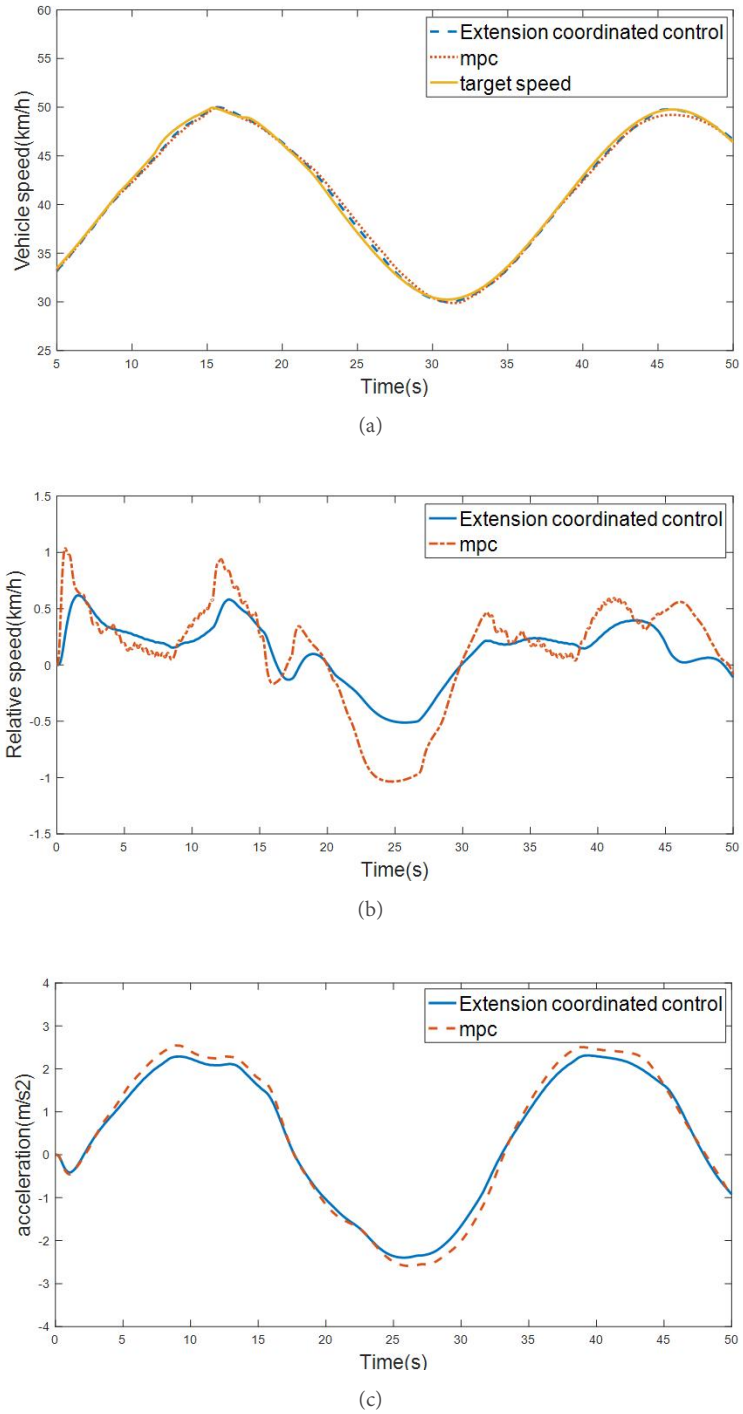

Figure 11. Simulation results of working condition No.3.a: condition No.3 vehicle speed; b: condition No.3 relative speed; c: condition No.3 acceleration.

5. DISCUSSION

When the traditional MPC is working under straight road conditions and the following distance between two vehicles is kept within the expected range, the risk of deterioration of ride comfort and fuel economy of the vehicle will be greatly increased. Therefore, the extension theory is introduced to construct the real-time weight matrix, and the weight coefficient of multiple targets is coordinated to improve other performance under the

premise of ensuring safety. This paper chooses the longitudinal following distance error of vehicles as the state vector and divides the classical, extendable, and non-domain based on an extension theory. According to different measurement modes, this paper selects different weight coefficient values to construct a real-time variable weight matrix. The simulation results of target vehicle speed tracking effects and acceleration change ranges show that the performance of the ACC vehicle controlled by an extension theory under the three working conditions is optimized compared with that controlled by the traditional MPC. This means that this control method can improve the ride comfort and fuel economy of the vehicle to achieve multi-target ACC.

This paper has several limitations:(1) In vertical control, selecting only one state variable for optimization cannot fully utilize the advantages of the extension theory; (2) The difference between simulated working conditions is not particularly significant: it cannot represent an optimization effect on the actual vehicle. In future research, the lateral stability of the vehicle should be further investigated, the horizontal and longitudinal joint MPC control should be established, and extension coordinated control theory should be utilized to change the weighted matrix coefficients in real time to adapt to curved driving conditions.

DECLARATIONS

Acknowledgments
This work was funded by the Natural Science Foundation of China (Grant No. 52275082) and the Fundamental Research Funds for the Central Universities QNXM20220029 and FRF-TP-20-037A2.

Authors' contributions
Made substantial contributions to the conception and design of the study and performed data analysis and interpretation: Li Z, Zhao X, Yang J Performed article typography: Liu M

Availability of data and materials
Not applicable.

Financial support and sponsorship
None.

Conflicts of interest
All authors declared that there are no conflicts of interest.

Ethical approval and consent to participate
Not applicable.

Consent for publication
Not applicable.

Copyright
© The Author(s) 2023.

REFERENCES

1. Yin S, Yang C, Kawsar I, Du H, Pan Y. Longitudinal predictive control for vehicle-following collision avoidance in autonomous driving considering distance and acceleration compensation. *Sensors* 2022;22:7395. DOI
2. Liu L, Zhang Q, Liu R, Zhu X, Ma Z. Adaptive cruise control system evaluation according to human driving behavior characteristics. *Actuators* 2021;10:90. DOI

3. Qu T, Zhao J, Gao H, Cai K, Chen H, Xu F. Multi-mode switching-based model predictive control approach for longitudinal autonomous driving with acceleration estimation. *IET Intell Transp Syst* 2020;14:2102-12. DOI
4. Wang H, Liu B, Ping X, An Q. Path tracking control for autonomous vehicles based on an improved MPC. *IEEE Access* 2019;7:161064-73. DOI
5. Vasebi S, Hayeri YM, Saghiri AM. A literature review of energy optimal adaptive cruise control algorithms. *IEEE Access* 2023;11:13636-46. DOI
6. Wang H, Sun Y, Gao Z, Chen L. Extension coordinated multi-objective adaptive cruise control integrated with direct yaw moment control. *Actuators* 2021;10:295. DOI
7. Zhao WZ, Fan ML, Wang CY, Jin Z, Li Y H∞/extension stability control of automotive active front steering system. *Mech Syst Signal Process* 2019;115:621-36. DOI
8. Wang H, Cui W, Xia Z, Jiang W. Vehicle lane keeping system based on TSK fuzzy extension control. *Proceedings of the Institution of Mechanical Engineers, Part D: Journal of Automobile Engineering* 2020;234:762-73. DOI
9. Chen J, Zhou Y, Liang H. Effects of ACC and CACC vehicles on traffic flow based on an improved variable time headway spacing strategy. *IET Intell Transp Syst* 2019;13:1365-73. DOI
10. Bai Y, Zheng Y, Liu S. Study on charging performance of solar panels auxiliary batteries for Hainan electric bus. *IOP Conf Ser: Mater Sci Eng* 2019;563:022031. DOI
11. Yu S, Sheng E, Zhang Y, Li Y, Chen H, Hao Y. Efficient nonlinear model predictive control of automated vehicles. *Mathematics* 2022;10:4163. DOI
12. Buerger J, Cannon M, Kouvaritakis B. An active set solver for input constrained robust receding horizon control. *Automatica* 2014;50:155-61. DOI
13. Yuan L, Zhao H, Chen H, Ren B. Nonlinear MPC-based slip control for electric vehicles with vehicle safety constraints. *Mechatronics* 2016;38:1-15. DOI
14. Guo L, Ge P, Sun D, Qiao Y. Adaptive cruise control based on model predictive control with constraints softening. *Appl Sci* 2020;10:1635. DOI
15. Wei L, Wang X, Li L, Fan Z, Dou R, Lin J. T-S fuzzy model predictive control for vehicle yaw stability in nonlinear region. *IEEE Trans Veh Technol* 2021;70:7536-46. DOI
16. Bai G, Liu L, Meng Y, Luo W, Gu Q, Ma B. Path tracking of mining vehicles based on nonlinear model predictive control. *Appl Sci* 2019;9:1372. DOI
17. Guo L, Ge P, Qiao Y, Xu L. Multi-objective adaptive cruise control strategy based on variable time headway. *IEEE Intelligent Vehicles Symposium(IV)* 2018;6:203-8. DOI
18. Wi H, Park H, Hong D. Model predictive longitudinal control for heavy-duty vehicle platoon using lead vehicle pedal information. *Int J Automot Technol* 2020;21:563-9. DOI
19. Lin F, Chen Y, Zhao Y, Wang S. Path tracking of autonomous vehicle based on adaptive model predictive control. *Int J Adv Robot Syst* 2019;16:1729881419880089. DOI
20. Zeng D, Yu Z, Xiong L, et al. HFO-LADRC lateral motion controller for autonomous road sweeper. *Sensors* 2020;20:2274. DOI
21. Song CJ, Jia HF. Car-following model optimization and simulation based on cooperative adaptive cruise control. *Sustainability* 2022;14:14067. DOI
22. Zhang D, Li K, Wang J. A curving ACC system with coordination control of longitudinal car-following and lateral stability. *Veh Syst Dyn* 2012;50:1085-102. DOI
23. Yan M, Chen W, Wang Q, Zhao L, Liang X, Cai B. Human-machine cooperative control of intelligent vehicles for lane keeping-considering safety of the intended functionality. *Actuators* 2021;10:210. DOI
24. Yang L, Mao J, Liu K, Du J, Liu J. An adaptive cruise control method based on improved variable time headway strategy and particle swarm optimization algorithm. *IEEE Access* 2020;8:168333-43. DOI
25. Wang X, Chen J, Quan S, Wang YX, He H. Hierarchical model predictive control via deep learning vehicle speed predictions for oxygen stoichiometry regulation of fuel cells. *Appl Energy* 2020;276:115460. DOI
26. Gao B, Cai K, Qu T, Hu Y, Chen H. Personalized adaptive cruise control based on online driving style recognition technology and model predictive control. *IEEE Trans Veh Technol* 2020;69:12482-96. DOI
27. Zhang W. A robust lateral tracking control strategy for autonomous driving vehicles. *Mech Syst Signal Process* 2021;150:107238. DOI
28. Tan Y, Zhang K. Real-time distributed cooperative adaptive cruise control model considering time delays and actuator lag. *Transp Res Rec* 2022;2676:93-111. DOI
29. He D, Peng B. Gaussian learning-based fuzzy predictive cruise control for improving safety and economy of connected vehicles. *IET Intell Transp Syst* 2020;14:346-55. DOI